Shear Layer Effect on Edge Flame Structure in a Non-Premixed Methane-Air Flame

R. B. McCoy,* H. N. Najm, J. Ray
Sandia National Laboratories,
Livermore, CA, USA

Abstract

We present a numerical study of the detailed structure of an edge flame in a laminar 2D non-premixed methane-air jet. A coupled Lagrangian-Eulerian low-Mach number numerical scheme using the GRImech1.2 $C_1 C_2$ chemical mechanism was applied. We analyze the effect of the strain-rate field on the structure and development of the edge flame by investigating two jet shear layer conditions with the jet fuel stream faster/slower than the coflow air stream. We show that the shear layer affects the edge flame orientation and the stretching of the lean and rich premixed branches, while the mixing layer defines edge flame internal structure, topology and position relative to the stoichiometric mixture fraction line. The ignition, development and branch folding of the edge flames is discussed and presented, as well as their detailed chemical structure.

Introduction

Edge flames can exist in many practical configurations where pockets of rich and lean mixtures coexist in close proximity and where partial premixing of fuel and oxidizer occurs. They are generally composed of three reaction zones (branches): a lean premixed branch, a rich premixed branch and a nonpremixed - diffusion flame branch; hence they are also known as triple or tribrachial flames. The two premixed branches form curved fronts behind which a diffusion flame develops and stabilizes. In the straining field the flame branches are distorted and for sufficiently high strain rates, one of the premixed branches can be extinguished or folded onto the diffusion tail, while the other branch continues to burn. For that reason the term 'edge flame' and not 'triple flame' seems more suitable.

There has recently been a growing number of experimental, analytical and numerical studies of edge flames, jet flame liftoff and stabilization [1–3], and on the propagation speed of edge flames [4–7]. Methane-air triple flames in particular were studied experimentally [8, 9] and numerically with a reduced chemical mechanism [10]. The triple flame folding mechanism by a vortex or a pair of vortices was suggested by Veynante *et al.* [11], also described in Reutsch *et al.* [4].

In our study we wish to examine the developing edge flame structure in straining flow fields and to understand the mechanism that determines the number of branches evident in an edge flame. To better understand the development of edge flames, and to examine the effect of the velocity field, we study two flow conditions with different flow fields, one with faster jet fluid and the other with faster coflow. In both cases the lean premixed wing survives and the rich premixed wing is folded onto the diffusion tail. This shows the numerical evidence of branch folding and it's mechanics. We examine the role of the mixing layer and the shear layer on the developing flame, and present the detailed chemical structure of the edge flame.

Formulation And Numerical Scheme

An Eulerian-Lagrangian low Mach number reacting 2D flow model with normal gravity was used in the simulations. The details of the model formulation and numerical scheme can be found in [12–15]. An Eulerian formulation of the energy and species conservation equations discretized on a multi-layered adaptive mesh is employed. The Lagrangian vortex method is adopted for the momentum equations, and an adaptive fast multipole method is used for the velocity evaluations. Since the domain of interest is open, the spatially uniform stagnation pressure is assumed to be constant in time. We also assume that the mixture has zero bulk viscosity and is a perfect gas. N_2 is regarded as dominant (as it is in fact for the mixture conditions investigated) such that the diffusion of any species in the mixture is approximated by binary diffusion into N_2 at the local temperature. Soret and Dufour effects and radiant heat transfer are neglected. The GRImech1.2 [16] $C_1 C_2$ chemical mechanism is used, with 32 species and 177 reactions. A second-order upwind Godunov scheme is used for spatial discretization of convective terms. A coupled Lagrangian-Eulerian time integration approach is adopted based on a second-order Runge-Kutta predictor-corrector formulation for both the Lagrangian and Eulerian integrations. The overall solution proceeds with global Lagrangian time steps, within which are embedded Eulerian sub-steps. Operator splitting is used within the Eulerian sub-steps to allow efficient computations with detailed

chemical source terms. An ODE integrator (CVODE) [17] was used to integrate the stiff chemical source terms.

Numerical Configuration Description

We compute the ignition and stabilization of a 2D laminar non-premixed methane jet with coflow air. The methane stream is diluted 40% (by volume) with N_2, the domain size is 10 cm$\times$5 cm. The mesh cell sizes range from 1 mm to 15 μm, from the coarsest to the finest mesh respectively. Boundary conditions include inflow at the bottom boundary, slip vertical walls, and an outflow top edge.

The flowfield is initialized with parallel streams of room-temperature air and N_2 diluted CH_4 and then allowed to relax to a steady jet solution. The ignition is then initialized by transient heating of a small spot in the jet mixing layer 1 cm above the jet inlet for the duration of 1 ms. We study two configurations: case A with jet stream velocity of 0.8 m/s and coflow air velocity of 0.25 m/s, and case B with fuel velocity of 0.25 m/s and coflow velocity of 0.8 m/s. The two cases studied are shown in Fig.1, where only the left half of the domain is presented (5 cm $\times$ 5 cm). The left column shows case A and the right column - case B, 4 ms after ignition started. The mole fraction of CH_4 is shown in color, the yellow line represents the stoichiometric mixture fraction line and the heat release rate for the flame fronts is shown as black contours. Studying these two configurations enables us to analyze the effect of the shear layer structure (faster fuel or oxidizer), and associated strain-rate fields, on the developing edge flame structure.
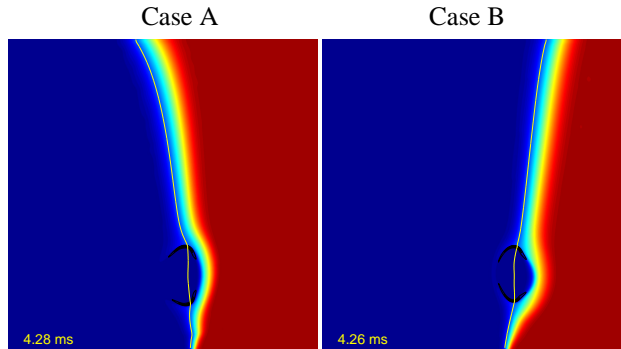

Fig. 1. The two cases studied: case A is shown in the left column and case B in the right; the mole fraction of CH_4 (color), the black contours represent heat release rate and the yellow line is the stoichiometric mixture fraction line. The color map: blue is mapped to the lowest value, red to the highest.

A mixture fraction is defined as in Bilger [18]

$$\xi^e = \frac{2Z_C/W_C + Z_H/(2W_H) + (Z_{O,2} - Z_O)/W_O}{2Z_{C,1}/W_C + Z_{H,1}/(2W_H) + Z_{O,2}/W_O},$$

where subscripts 1 and 2 refer to fuel and oxidizer streams respectively, and W_i is molar weight for species i. Subscripts C, H, O refer to carbon, hydrogen and oxygen. Z_i is an elemental mass fraction, and denotes the ratio between the mass of an element i and the total mass,

$$Z_i = \sum_{j=1}^{S} \mu_{ij} w_j, \qquad i = 1, ..., M$$

where S is the number of species and M total number of elements in the mixture, coefficients μ_{ij} denote the mass proportion of the elements i in the species j and w_j is the mass fraction for species j. The stoichiometric value of the mixture fraction is equal to $\xi^e_{stoich} = 0.17$ for this simulation.

Results and Discussion

The ignition process is presented in Fig.2, shown using the time evolution of the heat release rate. The yellow line represents the stoichiometric mixture fraction line. The top/bottom row corresponds to case A/B.
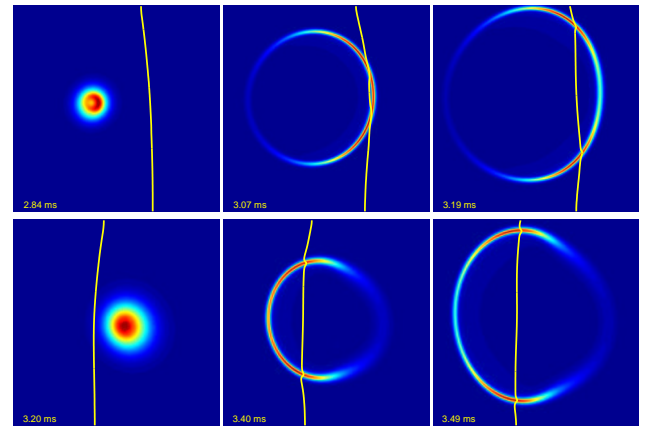

Fig. 2. Ignition process presented as time evolution of heat release rate (color); the yellow line is the stoichiometric mixture fraction line. The top row corresponds to case A and the bottom to case B. The dimensions of the region shown are 6 mm $\times$ 5 mm. Time is measured from the inception of heating for ignition.

In case A, ignition was initiated in the lean premixed zone to the left of the stoichiometric mixture fraction line, while in case B ignition was started in the fuel rich region. In both cases the ignition front forms a circular front that grows and propagates through the stoichiometric mixture fraction line. The lateral propagation of the front subsides as it reaches zones of very high or very low equivalence ratio deep into the jet or into the coflow. What is left over are two edge flames propagating up and down the stoichiometric mixture fraction line. It is evident from these plots

that although the two ignitions were started in two different regions, and at a different distances from the stoichiometric mixture fraction line, the two cases develop very similar flame fronts. The flame fronts develop in roughly the same rate (similar sizes of circular fronts), but in case A the front touches the mixture fraction line later then in case B, and the flame front is bigger in case A at the time it first touches the line. The middle column plots show the differences due to the different distance of the ignition spot from the stoichiometric mixture fraction line in the two cases. At the later time, the overall chemical structure, topology and propagation of the ignition fronts, when viewed relative to the stoichiometric mixture fraction line, is similar for the two studied cases, and is independent of the ignition origin and the strain rate distribution. Note that in both cases the extent of the lean premixed branch is much bigger then the rich premixed branch (the right column in Fig. 2).

The edge flames initially develop a triple branch structure, at least as far as the global structure of the heat release rate field is concerned, as shown in Fig.3 for several different time instances. Case A is shown in the top row and case B in the bottom. The edge flame structure consists of lean (on the left) and rich (on the right) premixed flame zones and the diffusion flame zone behind the premixed wings.
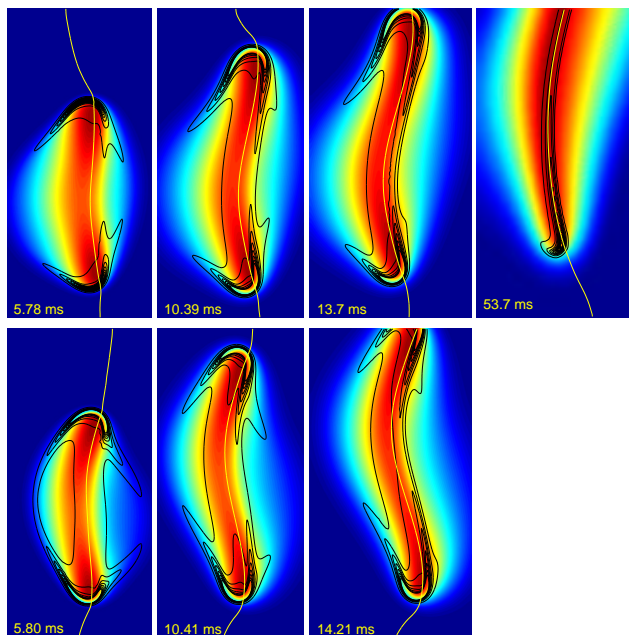

Fig. 3. Evolution of the edge flames; contours represent heat release and the color field depicts mole fraction of CO_2. The top row corresponds to case A and the bottom to case B. Heat release contours near the maximum are not shown, so as to not obstruct the view. The thin yellow line is the stoichiometric mixture fraction line. The frame dimensions are 0.8 cm × 1.75 cm.

The maximum heat release rate is located in the lean pre-

mixed zone, in agreement with the observation in hydrogen-air triple flames [7]. One can also observe that the heat release rate initially outlines the lean and rich premixed wings (frames corresponding to ∼5.8 ms). However, at later time, the rich branch of heat release rate contours aligns along the fuel-side of the diffusion flame (frames corresponding to ∼14 ms). The edge flame's rich branch becomes very small, folds onto the trailing diffusion branch, and nearly disappears. This is due to a much bigger equivalence ratio gradient (encountered immediately in front of the edge flame) on the rich side than on the lean side. Hence, on the rich side of the edge flame the flammability limit is more quickly met, and the rich premixed branch terminates.
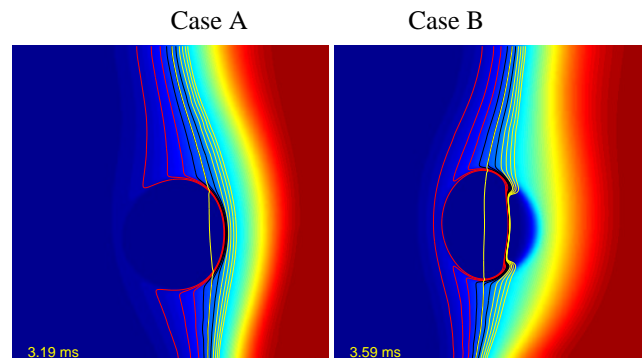

Fig. 4. The equivalence ratio isocontours in the beginning of ignition for both cases are shown as red, black and yellow contours, the middle black contour corresponds to the equivalence ratio of 0.5. The mole fraction of CH_4 is presented in color. The frame size is 6 mm × 5 mm.

We observe that the mixing layer is playing a crucial role in defining the structure of the flames, as in both cases the topology of the flames is such that the extent of the rich premixed branch is shorter then the lean premixed branch (last column in Fig.2) and is eventually folded onto the diffusion flame (Fig.3). The reason for that can be seen in Fig.4 where the equivalence ratio isocontours are shown as red, black and yellow lines, with the middle black line corresponding to the equivalence ratio equal 0.5. The plots depict the situation just after the ignition (∼3.5 ms). The red lines indicate leaner mixture and the yellow lines richer mixture. Given the uniform spacing of the contour line values, it is clear that gradients of the mixture fraction are much higher on the rich side than on the lean side, hence the flame structure extends more into the oxidizer side. The uneven gradients are defined by stoichiometry of the mixture and enhanced by the divergence of isocontours due to the flame front.

Figure 5 presents the equivalence ratio isocontours for the developing edge flame in case A for two times corresponding to the first and third column plots in the top row of Fig. 3 . The zoom into the bottom flame front is presented. It shows that the equivalence ratio gradients on the rich side increase with time, and the rich branch gets more

and more folded onto the diffusion flame, manifesting the branch folding mechanism in triple flames.
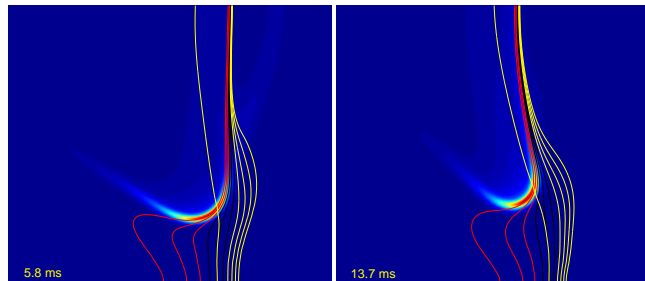

Fig. 5. The equivalence ratio isocontours for case A are shown. The heat release is plotted in color and the yellow line in the middle of the ignition zone is the stoichiometric mixture fraction line. The frame size is 8 mm × 8 mm.

The lower flame travels first downwards towards the jet inlet, but eventually is blown away and very slowly moves upwards with the velocity of 2.1 cm/s in case A and 3.5 cm/s in case B. The flame burning speed is 30.3 cm/s in case A and 31.5 cm/s in case B. The laminar premixed-flame burning speed S_L for the mixture used in the simulations is about 25.5 cm/s.
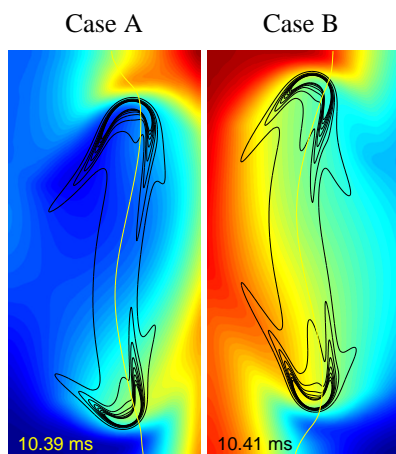

Fig. 6. Vertical velocity fields for case A (left), and case B (right). The structure and position of the flame is represented with heat release contours in black and a yellow stoichiometric mixture fraction line.

The vertical velocity fields corresponding to cases A and B are shown in Fig. 6. The shear layer structure causes different tilting of the edge flames in the two cases and induces stretching on the edge flame, but does not affect the internal flame chemical structure. The edge flames in both cases exist on the oxidizer side. The mixing layer defines the structure, topology and position (relative to the stoichiometric mixture fraction line) of the edge flame. The tilting and stretching induced by the shear layer and associated strain rate fields can be seen in the figure. Upward stretching of the rich side of the lower edge flame is seen in case A, whereas in case B the lean side of the lower edge flame is stretched, affecting the extent of the lean premixed branch.

The shear layer does not affect the topology and internal structure of the edge flame, and so the comparison of shape and structure of the mole fractions and production rates between the two strain-rate field cases did not reveal significant differences. In what follows we will focus our discussion on chemical structure of the propagating edge flame in one case only, namely on the case A with the jet fuel stream faster then the coflow air stream., and we will show the edge flame structure for time instance ∼19 ms after ignition.
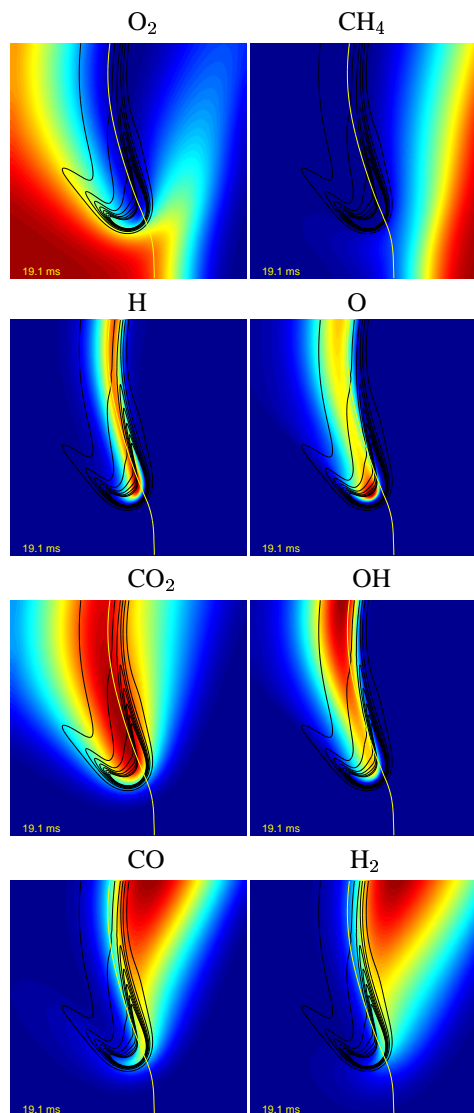

Fig. 7. The mole fraction of O_2, CH_4, H, O, CO_2, OH, CO, H_2 are presented in color. The structure and position of the flame is represented with heat release contours in black, and a yellow stoichiometric mixture fraction line. Domain height is ∼1cm.

4

Examination of the mole fraction fields of various species in the edge flame region brings up several points of interest. We observe significantly more penetration of O_2 around the edge flame and into the fuel (CH_4) stream than the converse, as seen in Fig. 7. Similar penetration by the oxidizer stream is observed in triple flames in methane [10], methanol [6] and hydrogen [19]. Note that this observation is consistent with the above reported smaller extent of the rich branch, as the concentration of CH_4 rises very quickly on the rich side of the edge flame, such that a higher equivalence ratio is reached faster than on the lean side, despite the more extensive penetration of O_2 into the fuel stream. As can be seen in Fig. 7, H, O, and CO_2 have localized peaks in the edge flame tip region, whereas OH peaks far downstream in the diffusion flame region. We observe a predominance of CO and H_2 on the rich side of the flame. Analysis of the structure of the diffusion flame a short distance (0.6 cm) behind the edge flame tip indicates that CH_4 and O_2 are available on the fuel and air sides respectively, with some O_2 premixing on the fuel-side of the flame. CH_4 and O_2 diffuse and react together in the diffusion flame.

We find that H_2O_2 and HO_2 radicals are predominant at the leading edge of the lean premixed edge-flame branch (Fig. 8). On the other hand, C, CH, CH_2 and CH_2^* concentrations are all aligned in a narrow strip on the fuel-side of the diffusion flame. C_2H_2 - a key soot precursor, is also predominant on the fuel-side of the flame, as might be expected, and peaks far downstream on the fuel-side in the diffusion flame region, as can be seen in Fig. 8 . Similarly C_2H_4 and C_2H_6, relatively stable species, are on the fuel-side, but extend further into it, with highest C_2H_6 near the rich premixed flame zone, whereas C_2H_4 peaks farther downstream near diffusion flame, more like C_2H_2. As for C_2H_3 and C_2H_5, which are very short lived, less stable species, they exist in narrow strips on the rich side of the edge flame. Their narrow-strip topology reflects the unstable nature of these radicals, and is consistent with their characteristic structure in a premixed methane-air flame. CH_2O wraps around and peaks in the leading front of the edge flame and extends far into the fuel-side of the flame.

The species production rates will not be shown due to space constraint, but we will discuss them in detail below. All the species are consumed or produced predominantly in the premixed flame zone and most of them peak in the lean premixed flame front, except for H_2 and CO that peak in the rich premixed edge flame branch. O, CO_2, OH and also H_2O production contours are largely confined to the lean side of the premixed front. The consumption of OH and O extends from lean to rich premixed zone and into the diffusion flame zone.
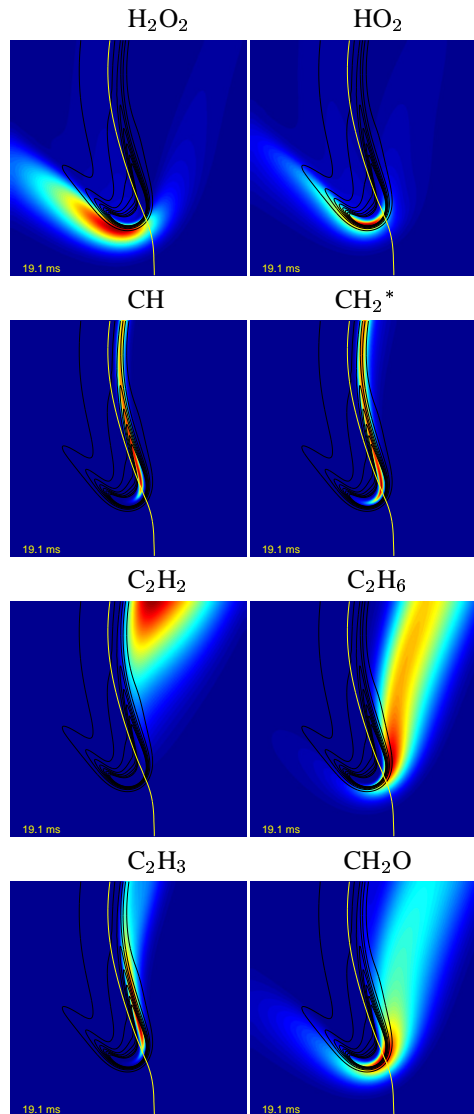

Fig. 8. The mole fraction of H_2O_2, HO_2, CH, CH_2^*, C_2H_2, C_2H_6, C_2H_3, and CH_2O are presented in color. The structure and position of the flame is represented with heat release contours in black, and a yellow stoichiometric mixture fraction line. Domain height is $\sim$1cm.

We observe that H_2O_2 is produced on the leading edge of the edge flame in the cold region and consumed in its immediate downstream vicinity, and it's structure lays mainly on the lean side of the premixed zone. HO_2 structure is similar but does not extend as far in front of the edge flame. CH, CH_2 and CH_2^* production rates peak in the premixed zone of the edge flame and extend into the diffusion flame region, aligned in the narrow strip on the rich side of the diffusion flame. C_2H structure is very similar but peaks higher in the diffusion flame zone. C_2H_2, reveals very different reaction rate structure, much wider and with the peak consumption and production far downstream in the diffusion flame region. Its topology extends more into the rich side of the

5

flame. C_2H_6 as well as C_2H_5 and C_2H_4 production rate profiles extend from the lean to rich premixed flame fronts, whereas C_2H_3 production is confined mostly to the rich premixed flame zone and extends into the diffusion flame rich side, similar for C_2H_2 and C_2H. CH_2O is produced on the leading edge of the premixed fronts, both lean and rich side.

Conclusions

Edge flame structure and topology in a 2D laminar methane-air jet was studied numerically and experimentally. Ignition in the computed jet mixing layer was achieved by localized heating, creating a circular premixed flame front that rapidly grows and moves toward the stoichiometric mixture fraction line, penetrates it, and propagates along it, forming two edge flame structures that move up and down the line. Two different cases were studied, case A with faster jet fluid and case B with faster coflow. The motivation for studying these two configurations was to investigate the effect of the velocity field on the structure and development of edge flames, thereby discriminating between shear layer and mixing layer roles in defining edge flame structure. Despite the flow-field differences, the developed edge flames do not show significant difference in internal structure. The heat release contours initially span lean and rich premixed flame branches, but eventually the rich branch of heat release rate contours aligns along the rich side of the diffusion flame edge, and becomes very small. This is shown to be consistent with the uneven equivalence ratio variation on the lean and the rich sides immediately in front of the leading edge of the flame. The high equivalence ratio gradient on the rich side causes burning to quickly subside with distance from the stoichiometric mixture fraction line, and shows the mechanism by which the rich premixed branch gets folded onto the diffusion flame. The maximum heat release rate is located on the lean side in both cases. The shear layer affects the edge flame orientation and the stretching of the lean and rich premixed branches, while the mixing layer defines edge flame internal structure, topology and position relative to the stoichiometric mixture fraction line.

Acknowledgements

References

[1] Muñiz, L., and Mungal, M.G., *Combustion and Flame*, 111:16–31 (1997).

[2] Lee, B.J., and Chung, S.H., *Combust. Flame*, 109:167 (1997).

[3] Ghosal, S., and Vervisch, L., *Combust. Flame*, 123:646 (2001).

[4] Reutsch, G.R., Vervisch, L., and Liñán, A., *Phys. Fluids*, 7(6):1447–1454 (1995).

[5] Daou, J., and Liñán, A., *Combust. Theory Modelling*, 2:449–477 (1998).

[6] Echekki, T., and Chen, J., *Combustion and Flame*, 114:231–245 (1998).

[7] Im, H.G., and Chen, J.H., *Combust. Flame*, 126:1384 (2001).

[8] Mueller, C.J., and Schefer, R.W., *Proc. Comb. Inst.*, 27:1105–1112 (1998).

[9] Kioni, P.N., Bray, N.C., Greenhalgh, D.A., and Rogg, B., *Combust. Flame*, 116:192 (1999).

[10] Plessing, T., Terhoeven, P., Peters, N., and Mansour, M.S., *Combust. Flame*, 115:335 (1998).

[11] Veynante, D., Vervisch, L., Poinsot, T., Liñán, A., and Ruetsch, G., *Center for Turbulence Research, Proceedings of the Summer Program*, Stanford, CA, Stanford University, Stanford Univ., pp. 55–73, (1994).

[12] Najm, H.N., Schefer, R.W., Milne, R.B., Mueller, C.J., Devine, K.D., and Kempka, S.N., Technical Report SAND98-8232, Sandia National Labs., Alb., New Mexico, (1998).

[13] Devine, K., and Flaherty, J., *Appl. Numer. Math.*, 20:367–386 (1996).

[14] Ray, J., Najm, H.N., Milne, R.B., Devine, K.D., and Kempka, S.N., *Proc. Comb. Inst.*, 28:219–226 (2000).

[15] Najm, H.N., Milne, R.B., Devine, K.D., and Kempka, S.N., *ESAIM Proceedings*, volume 7, pp. 304–313, (1999).

[16] Frenklach, M., Wang, H., Goldenberg, M., Smith, G.P., Golden, D.M., Bowman, C.T., Hanson, R.K., Gardiner, W.C., and Lissianski, V., Top. Rep. GRI-95/0058, GRI, (1995).

[17] Brown, P.N., Byrne, G.D., and Hindmarsh, A.C., *SIAM J. Sci. Stat. Comput.*, 10:1038–1051 (1989).

[18] Bilger, R.W., Starner, S.H., and Kee, R.J., *Comb. and Flame*, 80:135–149 (1990).

[19] Im, H.G., and Chen, J.H., *Combust. Flame*, 119:436 (1999).